《原子核物理评论》
www.npr.ac.cn Nuclear Physics Review
Started in 1984

极深垒下熔合反应中扩散过程的研究

程凯旋　许昌

Investigation of Diffusion Process in Deep Sub-barrier Fusion Reactions

CHENG Kaixuan, XU Chang

在线阅读 View online: https://doi.org/10.11804/NuclPhysRev.37.2020039

引用格式:
程凯旋，许昌. 极深垒下熔合反应中扩散过程的研究[J]. 原子核物理评论，2020，37(4):809-815. doi: 10.11804/NuclPhysRev.37.2020039
CHENG Kaixuan, XU Chang. Investigation of Diffusion Process in Deep Sub-barrier Fusion Reactions[J]. Nuclear Physics Review, 2020, 37(4):809-815. doi: 10.11804/NuclPhysRev.37.2020039

第 37 卷 第 4 期 原 子 核 物 理 评 论 Vol.37, No.4
2020 年 12 月 Nuclear Physics Review Dec. , 2020

Article ID: 1007-4627(2020)04–0809–07

Investigation of Diffusion Process in Deep Sub-barrier Fusion Reactions

CHENG Kaixuan, XU Chang†

(*School of Physics, Nanjing University, Nanjing 210093, China*)

Abstract: We introduce a new diffusion factor to describe the hindrance phenomenon in fusion reactions at deep sub-barrier energies based on the Pauli blocking effect after the projectile and target overlap. In this approach, the fusion cross sections are assumed to be the product of two parts: the tunneling factor to overcome the Coulomb barrier and the diffusion factor after two colliding nuclei contact. The former is described by coupled-channels approach and the latter depends on the colliding energies as well as the temperature of system. In total, 21 fusion systems with hindrance phenomenon are analyzed in details and it is found that the diffusion factor plays an important role near the experimental threshold energies of fusion hindrance. In addition, taking negative-Q-value system ^{64}Ni+^{64}Ni and positive-Q-value system ^{24}Mg+^{30}Si as examples, not only fusion cross sections but also two important representations, namely, astrophysical S factor and logarithmic derivative, are found to be in good agreement with experimental data.

Key words: fusion hindrance; coupled-channels model; diffusion process

CLC number: O571.4 **Document code:** A **DOI:** 10.11804/NuclPhysRev.37.2020039

1 Introduction

The fusion reactions of heavy nuclei have been extensively investigated to understand the mechanism of quantum tunneling in complex many-body systems. The analysis of fusion reaction data provide very abundant information about the synthesis of new elements or superheavy nuclei to extend the periodic table. In heavy-ion fusion reactions, fusion takes place when the projectile penetrates through the Coulomb barrier, formed by the repulsive Coulomb interaction and an attractive nuclear interaction. When the colliding energy is near and above the Coulomb barrier, the one-dimensional potential model well reproduces the experimental fusion cross sections[1]. While at sub-barrier energies, the strong enhancement of fusion cross sections[2] demonstrates the necessity of including the coupled-channels (CC) effects which create a multidimensional potential barrier owing to the coupling of the relative motion to the nuclear intrinsic degrees of freedom of colliding nuclei[3]. Several CC codes have been successfully applied to achieve the description of fusion cross sections[4–8].

Recently, at the colliding energies far below the Coulomb barrier, an unexpected steep falloff feature of the experimental fusion cross sections in contrast to the theoretical prediction has generated renewed interest to further explore the fusion theory[9]. This steep falloff feature in experimental data, also called "fusion hindrance", is hard to explain by the CC model[10]. To describe this fusion hindrance at the overlapping region, two approaches with different assumptions have been proposed[11–15]. One is the sudden approach proposed by Mişicu and Esbensen[11–15], which assumes that the fusion reactions occur rapidly with the fixed densities of two colliding nuclei and there is a strong repulsive core at the overlapping region owing to the saturation properties of nuclear matter. The other is the adiabatic approach proposed by Ichikawa *et al.*[14–15], which assumes that after the contact of projectile and target, an elongated composite system with the optimized density distribution is formed and the CC effect gradually damps owing to the diminishing of the excitation strengths of the target/projectile vibrational states[16–17]. By employing different potentials and reasonable parameters, the fusion cross sec-

Received date: 23 Jun. 2020; **Revised date:** 23 Jul. 2020

Foundation item: National Natural Science Foundation of China(11822503, 11575082); Fundamental Research Funds for Central Universities(Nanjing University)

Biography: CHENG KaixuanCHENG Kaixuan(1991–), male, Xinxiang, Henan, Ph.D, working on theoretical nuclear physics; E-mail: Kaixuan_c@163.com

† **Corresponding author:** XU Chang, E-mail: cxu@nju.edu.cn.

tions calculated by these two models at deep sub-barrier energies are in good agreement with the experimental data[12, 15]. In addition, other theoretical works have also been devoted to investigating the density overlap in fusion reactions[18–29].

In our recent work[28–29], a microscopic Pauli blocking potential due to the density overlap of two colliding nuclei is introduced into the fusion reactions and describes the fusion hindrance well for reactions $^{16}\mathrm{O}+^{208}\mathrm{Pb}$, *etc.* This Pauli blocking potential is obtained by solving the in-medium four-nucleon wave equation with a variational approach[30] and has been successfully applied into the radioactive α-cluster decay in heavy nuclei and superheavy nuclei[31–33]. In literatures[30, 34], Röpke, *et al.* concluded that the α particle is very sensitive to the Pauli blocking from surrounding matter and at the density overlap region, the α particle dissolves and its four nucleons diffuse into single-particle states. Translated to the fusion case, this means that two nuclei approaching each other stay compact almost elementary particles until their density overlaps. After overlap, the strong Pauli blocking makes two colliding nuclei dissolve more or less and diffuse to form the compound nuclei.

So in this paper, a phenomenological diffusion factor due to the Pauli blocking after two colliding contact is introduced to explore the fusion hindrance at deep sub-barrier energies. In total, 21 fusion systems in which the fusion hindrance has been observed are analyzed in details. In order to better understand the diffusion process, a systematic investigation of not only the fusion cross sections but also the astrophysical S factor and logarithmic derivative representations is made for two typical fusion systems $^{64}\mathrm{Ni}+^{64}\mathrm{Ni}$ (with negative Q value) and $^{24}\mathrm{Mg}+^{30}\mathrm{Si}$ (with positive Q value).

The rest of paper is organized as follows. In Sec. 2, we present the CC model and specify the expression of diffusion factor used in the calculations. In Sec. 3, a systematic comparison of the fusion cross section, astrophysical S factor, and logarithmic derivative by considering the diffusion factor are made with the experimental data. In addition, 21 systems with fusion hindrance are analyzed. The summary is displayed in Sec. 4.

2 Theoretical framework

At above and sub-barrier energies, overcoming the Coulomb barrier between two colliding nuclei leads automatically to the formation of the compound nucleus, *i.e.*, the fusion occurs before projectile and target touching each other. With the decrease of the colliding energies, the fusion reaction takes place slowly and after contact the diffusion effect has a non-negligible influence on the tunneling process. Therefore, the fusion reaction is assumed to be consisted of tunneling effect and diffusion effect. The fusion cross section, $\sigma_{\rm fus}$, is then the product of the tunneling factor to overcome the Coulomb barrier, $\sigma_{\rm tun}$, and diffusion factor to form compound nucleus, $P_{\rm dif}$,

$$\sigma_{\rm fus}=\sigma_{\rm tun}\times P_{\rm dif}. \tag{1}$$

We apply the CCFULL code to calculate the tunneling factor[7, 35]. In the calculations, the incoming wave boundary condition (IWBC) is imposed and the absorption radius is taken to be at the minimum of the potential inside the Coulomb barrier[7, 35]. With the IWBC, the CC equations can be given by[7, 35]

$$\left[-\frac{\hbar^2}{2\mu}\frac{d^2}{dR^2}+\frac{J(J+1)\hbar^2}{2\mu R^2}+V(R)+\epsilon_n-E\right]u_n(R)+\sum_m V_{nm}(R)u_m(R)=0, \tag{2}$$

where E is the incident energy in the center-of-mass frame, ϵ_n is the excitation energy of the nth channel, and u_n is the radial wave function of the nth channel. The total potential $V(R)$ is consisted of both Coulomb and nuclear interactions between two colliding nuclei, *i.e.*, $V(R)=V_{\rm N}(R)+V_{\rm C}(R)$. In sudden and adiabatic models, the mechanisms and potentials involved after contact are totally different. Here, we simulate the Pauli blocking by introducing the diffusion factor, which is independent of the above two models.

The nuclear interaction $V_{\rm N}(R)$ used in calculations is the Akyüz-Winther nuclear potential given by[36]

$$V_{\rm N}(R)=-\frac{V_0}{1+\exp(\frac{R-R_0}{a})}, \tag{3}$$

where the depth of potential V_0 is obtained from[36]

$$V_0=16\pi\frac{R_{\rm P}R_{\rm T}}{R_{\rm P}+R_{\rm T}}\gamma a, \tag{4}$$

and the radius R_0 is written as $R_0=R_{\rm P}+R_{\rm T}$ in which the radius of colliding nucleus R_i is given by[36]

$$R_i=1.2A_i^{1/3}-0.09. \tag{5}$$

The surface energy coefficient γ and the diffuseness parameter a are written by[36]

$$\gamma=0.95(1-1.8I_{\rm P}I_{\rm T}), \tag{6}$$

$$a=\frac{1}{1.17[1+0.53(A_{\rm P}^{-1/3}+A_{\rm T}^{-1/3})]}, \tag{7}$$

respectively, where I_i denotes the relative neutron-proton excess of projectile or target nuclei. The Coulomb interaction $V_{\rm C}(R)$ is obtained from $V_{\rm C}(R) = Z_{\rm P}Z_{\rm T}e^2/R$. The symbol $V_{\rm nm}(R)$ denotes the matrix of coupling Hamiltonian which is calculated by the collective model with the Coulomb and nuclear components (for more detailed information, see Ref. [35] and references therein).

By solving the CC equations the penetrability P_J can be obtained and the tunneling factor $\sigma_{\rm tun}$ is then given by[35]

$$\sigma_{\rm tun}(E) = \frac{\pi}{k^2}\sum_J (2J+1)P_J(E), \tag{8}$$

where $k = \sqrt{2\mu E/\hbar^2}$ is the wave number associated with the energy E.

In what follows we focus attention on the Pauli blocking term, *i.e.*, diffusion factor describing the evolution of composite system after contact. In the synthesis of superheavy nuclei, such as cold fusion reactions, the strong overlap between two colliding nuclei leads to an obvious hindrance effect by bombarding ^{208}Pb and ^{209}Bi targets with ^{48}Ca, ^{50}Ti, ^{54}Cr, ^{58}Fe, ^{62,64}Ni and ^{70}Zn. To interpret this strong hindrance effect in cold fusion reactions, Świątecki, *et al.* introduced a diffusion factor in fusion-by-diffusion model[37–40] to describe the diffusion process from the contact of colliding nuclei to the formation of compound nucleus. By considering this statistical diffusion probability associated with the energy in units of the temperature of fusion system, the experimental cross sections with one neutron emitted from the compound nucleus can be described well[39].

Here, analogous to the diffusion process in the synthesis of the superheavy nuclei[37–40], a phenomenological diffusion factor is employed to describe the hindrance phenomenon in fusion reactions at deep sub-barrier energies. The diffusion factor is given by

$$P_{\rm dif}(E,T) = \begin{cases} 1, & E > E_{\rm d}, \\ \exp\left(-\dfrac{(E-E_{\rm d})^2}{T^2}\right), & E < E_{\rm d}, \end{cases} \tag{9}$$

where $E_{\rm d}$ denotes the initial energy of diffusion process given by $E_{\rm d} = V(R_{\rm d})$, $R_{\rm d}$ is the diffusing radius defined by $R_{\rm d} = r_{\rm d}(A_{\rm P}^{1/3} + A_{\rm T}^{1/3})$, and $r_{\rm d}$ can be obtained by fitting the experimental fusion cross sections. The symbol T in Eq. (9) is the temperature of fusion system related to the compound nuclei excitation energy $E^*_{\rm CN}$ or the colliding energy E and the Q-value in entrance channel[41–42]

$$E^*_{\rm CN} = E + Q = \frac{1}{9}AT^2 - T, \tag{10}$$

in which $A = A_{\rm P} + A_{\rm T}$ is the mass number of compound nucleus.

3　Results and discussion

In Fig. 1, we give the fusion cross sections for negative-Q-value system ^{64}Ni+^{64}Ni and positive-Q-value system ^{24}Mg+^{30}Si. All input parameters for the CC calculations are the same as those in Refs. [17, 43]. The experimental data denoted by solid circles are taken from Refs. [44–46]. The dotted and dashed lines indicate the results calculated without and with the CC effects, respectively. The solid line indicates the results calculated by CC model with the diffusion factor. The diffusing radius parameters $r_{\rm d}$ are 1.23 and 1.40 fm for fusion systems ^{64}Ni+^{64}Ni and ^{24}Mg+^{30}Si, respectively. Note that the experimental data at the deep sub-barrier energies are overestimated by the cal-

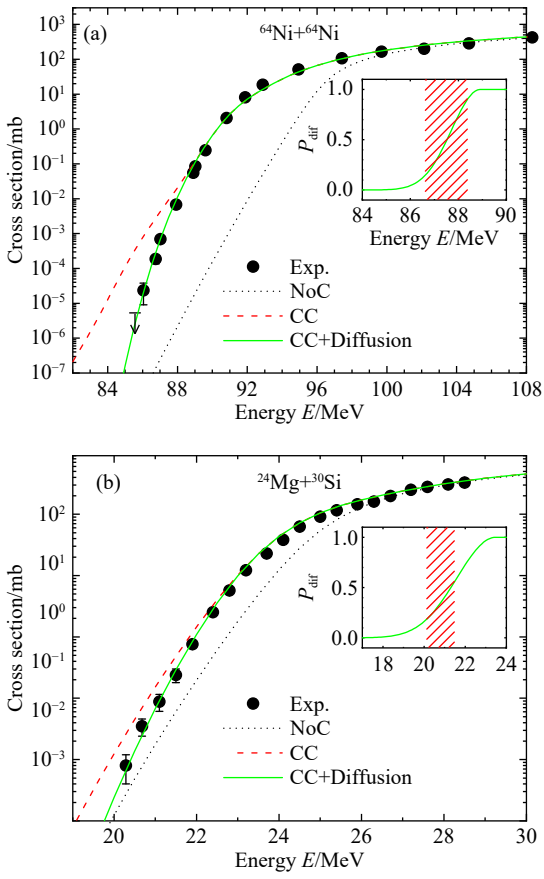

Fig. 1　(color online) The fusion cross sections for the (a) ^{64}Ni+^{64}Ni and (b) ^{24}Mg+^{30}Si systems. The solid circles denote the experimental data[44-46]. The dotted and dashed lines indicate the results calculated without and with the CC effects, respectively. The solid line indicates the results calculated by CC model with diffusion factor. The inset gives the corresponding diffusion factor and the shallow region denotes the experimental threshold energy.

culated cross sections only resulting from CC model. By considering the diffusion factor after the overlap of projectile and target, the calculated fusion cross sections have a rapid decrease at deep sub-barrier energies and describe the fusion hindrance well.

The insert in Fig. 1 shows the diffusion factors versus the incident energies. At high incident energies ($E > 88.93$ MeV for ^{64}Ni+^{64}Ni and $E > 23.51$ MeV for ^{24}Mg+^{30}Si), the compound nucleus is formed automatically once the Coulomb barrier is penetrated owing to the strong attractive nuclear force in the classical allowed region. Thus, the influence of diffusion process is week and the diffusion factor is assumed to be 1. With the decrease of incident energies, two colliding nuclei touch each other during the tunneling process and the diffusion process has a significant hindrance effect as shown in insert. In addition, the experimental threshold energy, the onset of fusion hindrance, is denoted by the shallow region. Notice that the diffusion factor plays a main role near the threshold energies.

Fig. 2 shows the astrophysical S factor and logarithmic derivative representations of the fusion cross sections for ^{64}Ni+^{64}Ni [44] and ^{24}Mg+^{30}Si [45–46] systems. The dashed and solid lines denote the results calculated by CC model without and with diffusion factor, respectively. In both systems, the results calculated with the diffusion factor have a significant improvement and are in good agreement with the experimental data. For comparison, in Fig. 2(a) and (b), the results calculated by using the sudden model from Ref. [11] and the adiabatic model from Ref. [15] are plotted by the dotted and dash-dotted lines, respectively. Because of totally different assumptions, two models have the diverse results at much deeper incident energies. For example, in Fig. 2(b) the logarithmic derivative resulting from adiabatic model is saturated below a certain incident energy and, conversely, the result of sudden model increases rapidly with decreasing energies. Interestingly, a hybrid result, which indicates the density variation may be simultaneous with the fusion reactions, is presented by

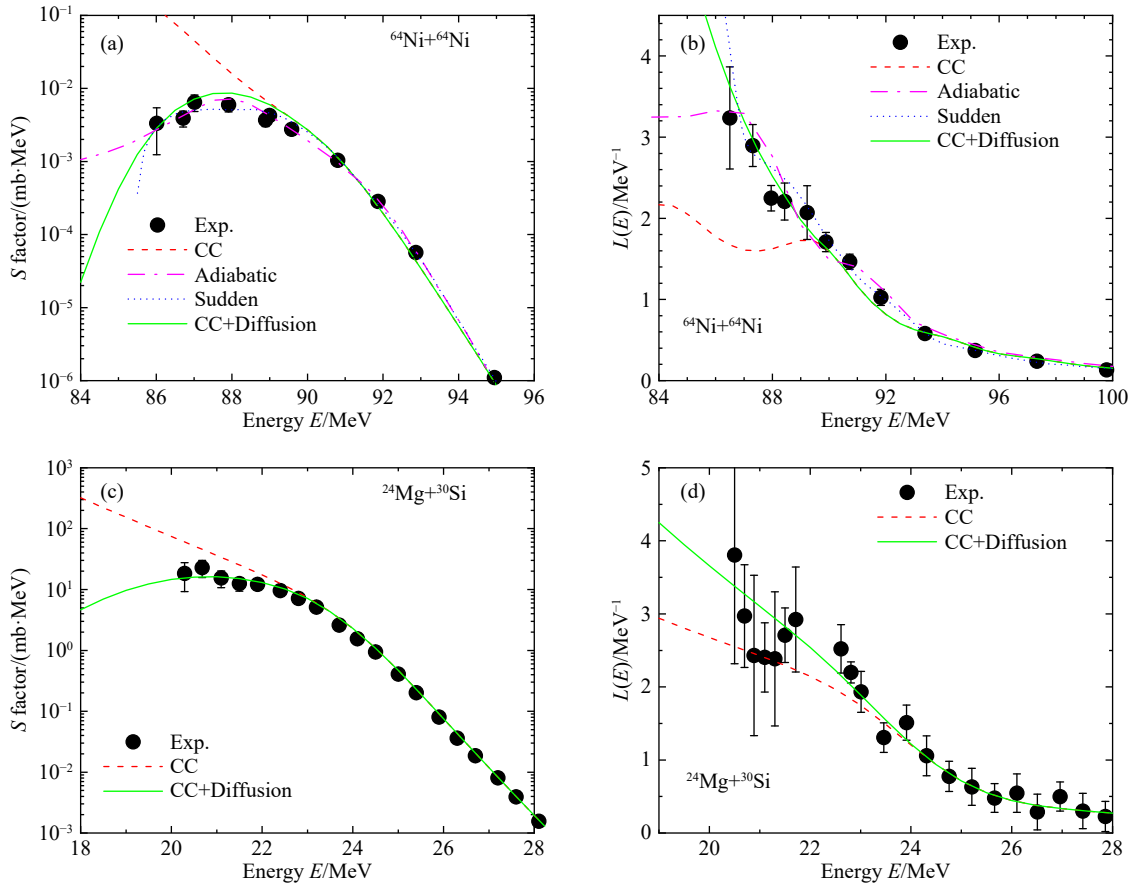

Fig. 2 (color online) Astrophysical S factor and logarithmic derivative representations of the fusion cross sections versus colliding energies for the ^{64}Ni+^{64}Ni and ^{24}Mg+^{30}Si fusion systems. The solid circles denote the experimental data[44-46]. The dashed and solid lines denote the results calculated by CC model without and with diffusion factor, respectively. In (a) and (b), the dotted and dot-dashed lines are the results calculated by using the sudden model[11] and the adiabatic model[20].

combining the CC approach and the diffusion process as shown in Fig. 2(a) and (b).

Next we extend the calculations to other 19 fusion systems in which the fusion hindrance phenomena are also observed. Table 1 specifies these fusion systems and summarizes all results of diffusing radius and initial energy. The third column, E_s, is the experimental threshold energy where the curve of S factor shows a maximum. The Q values of the entrance channel are listed in the fourth column. The symbols r_d, R_d and E_d are the diffusing radius parameters and the initial energies used in Eq. (9). Note that the energies E_d indicating the onset of the diffusion process for total 21 systems studied are almost consistent with the threshold energies of fusion hindrance E_s and this suggests that the fusion hindrance is strongly associated with the dynamic diffusion after the projectile and target overlap. The χ^2 values calculated by CC model without and with diffusing factors are given in the eighth and ninth columns, respectively. It is seen that a better fit is achieved by considering the diffusing factors. The last column is the references where the experimental fusion cross sections used in calculations and the corresponding threshold energies are taken.

Table 1　The radius and energy used in diffusing factor for the systems discussed in Refs. [43, 47]. The symbol A_{CN} denotes the mass number of the compound nuclei. The symbol E_s in the third column is the experimental threshold energies of fusion hindrance. The fourth column lists the Q value of the entrance channel. The symbols r_d, R_d and E_d are the diffusing radius and energy parameters used in Eq. (9). The eighth and ninth columns denote the χ^2 values of fusion cross sections calculated by CC model without and with diffusing factor, respectively. The last column is the references where the experimental fusion cross sections and threshold energies are taken.

System	A_{CN}	E_s /MeV	Q /MeV	r_d /fm	R_d /fm	E_d /MeV	χ_1^2/N	χ_2^2/N	Refs.
^{90}Zr+^{92}Zr	182	170.7±1.7	–153.7	1.14	10.26	171.16	214.5	11.92	[48]
^{90}Zr+^{90}Zr	180	175.2±1.8	–157.3	1.183	10.60	175.46	450.1	25.01	[48]
^{90}Zr+^{89}Y	179	170.8±1.7	–151.5	1.18	10.56	170.41	152.7	10.18	[48]
^{60}Ni+^{89}Y	149	122.9±1.2	–90.5	1.212	10.16	123.48	105.0	9.55	[9]
^{48}Ca+^{96}Zr	144	88.1±1.3	–45.9	1.25	10.27	90.63	60.96	59.17	[49]
^{64}Ni+^{64}Ni	128	87.5±0.9	–48.8	1.23	9.84	88.93	49.37	3.09	[44]
^{58}Ni+^{58}Ni	116	94.0±0.9	–65.8	1.238	9.58	93.69	4.13	1.77	[50]
^{40}Ca+^{90}Zr	130	91.9±0.9	–57.0	1.225	9.68	92.48	179.0	178.8	[51]
^{54}Fe+^{58}Ni	112	86.7±0.9	–56.5	1.24	9.48	87.04	14.22	2.07	[52]
^{34}S+^{89}Y	123	72.6±0.7	–36.6	1.265	9.75	73.89	1374	42.97	[53]
^{32}S+^{89}Y	121	73.1±0.7	–36.6	1.265	9.66	74.56	759.3	33.01	[53]
^{16}O+^{208}Pb	224	69.0±2.0	–46.5	1.25	10.32	67.87	1155	18.42	[18]
^{48}Ca+^{48}Ca	96	48.2±1.0	–2.98	1.31	9.52	48.60	9.59	5.41	[54]
^{40}Ca+^{48}Ca	88	47.0±0.5	4.56	1.285	9.06	48.31	90.75	90.65	[55]
^{40}Ca+^{40}Ca	80	48.0±1.0	–14.2	1.275	8.72	49.97	1.62	1.61	[56]
^{28}Si+^{64}Ni	92	45.6±0.5	–1.78	1.281	9.01	47.33	273.4	19.89	[57]
^{12}C+^{198}Pt	210	48.2±1.0	–14.0	1.218	10.06	48.27	14.20	10.39	[58]
^{11}B+^{197}Au	208	40.0±1.5	–5.0	1.252	10.07	40.73	9.95	9.03	[59]
^{28}Si+^{30}Si	58	24.2±3.6	14.3	1.37	8.42	26.62	5.25	3.85	[60]
^{24}Mg+^{30}Si	54	20.8±0.7	17.9	1.40	8.39	23.51	11.00	4.65	[45]
^{12}C+^{30}Si	42	10.5±0.75	14.1	1.38	7.45	10.38	6.98	5.31	[61]

In Fig. 3, the radius parameters in the diffusion factor versus the mass numbers of the compound nuclei are displayed. The circles denote the values of diffusing radius extracted from 21 fusion systems with Q value ranging from −157.3 to 17.9 MeV. The diffusing radius parameters r_d and R_d versus the mass number of compound nuclei are shown in Fig. 3(a) and (b), respectively. A good linear relationship between the diffusing radius and the mass numbers of compound nuclei is shown and the dashed line denotes the fitting result of all diffusing radius values obtained here. In addition, the stars are the distances of the closest approach evaluated with the time-dependent Hartree-Fock (TDHF) method and then the

dynamic diffusion process plays an important role in the synthesis of superheavy nuclei[62]. Note that the calculated results of our method agree with the prediction of TDHF method for superheavy nuclei.

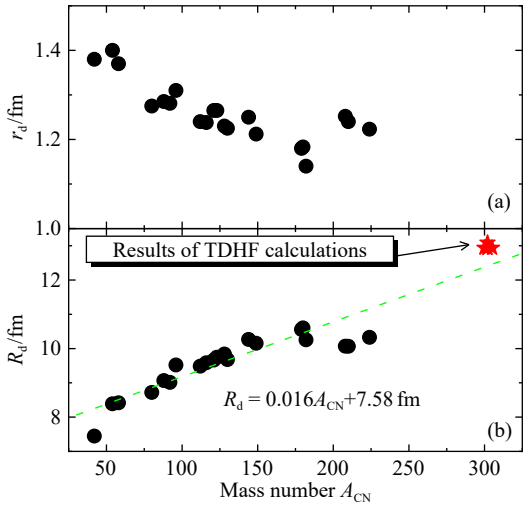

Fig. 3 (color online) The radius parameters in the diffusion factor versus the mass numbers of the compound nuclei for the systems listed in Table 1. The dashed line is a linear fitting result of all values obtained. The stars indicate the results of TDHF calculations in Ref. [62].

4 Summary

In summary, the influence of Pauli blocking effect on the fusion hindrance at deep sub-barrier energies is explained from the perspective of diffusion. After two colliding nuclei contact, there exits a strong blocking effect on the diffusion process to form the compound nucleus. By introducing a simple diffusion factor relied on the incident energy and the temperature of fusion system, the hindrance of fusion cross sections at deep sub-barrier energies for ^{64}Ni + ^{64}Ni and ^{24}Mg + ^{30}Si systems is described well. The astrophysical S factor and logarithmic derivative resulting from the tunneling and diffusion processes are also in good agreement with the experimental data. In addition, 21 fusion systems with fusion hindrance are analyzed and there is a consistency between the initial energies of diffusion process and the experimental threshold energies. This suggests that the diffusion process plays an important role near the threshold energies.

References:

[1] GUTBROD H H, WINN W G, BLANN M. Nucl Phys A, 1973, 213: 267.
[2] DASGUPTA M, HINDE D J, ROWLEY N, et al. Annu Rev Nucl Part Sci, 1988, 48: 401.
[3] BALANTEKIN A B, TAKIGAWA N. Rev Mod Phys, 1977, 70: 77.
[4] DASSO C H, LANDOWNE S. Comput Phys Commun, 1987, 46: 187.
[5] FERNÁNDEZ-NIELLO J, DASSO C H, LANDOWNE S. Comput Phys Commun, 1989, 54: 409.
[6] DASGUPTA M, NAVIN A, AGARWAL Y K. Nucl Phys A, 1992, 539: 351.
[7] HAGINO K, ROWLEY N, KRUPPA A T. Comput Phys Commun, 1999, 123: 143.
[8] NEWTON J O, MORTON C R, DASGUPTA M, et al. Phys Rev C, 2001, 64: 064608.
[9] JIANG C L, ESBENSEN H, REHM K E, et al. Phys Rev Lett, 2002, 89: 052701.
[10] HAGINO K, ROWLEY N, DASGUPTA M. Phys Rev C, 2003, 67: 054603.
[11] MIŞICU Ş, ESBENSEN H. Phys Rev Lett, 2006, 96: 112701.
[12] MIŞICU Ş, ESBENSEN H. Phys Rev C, 2007, 75: 034606.
[13] ESBENSEN H, MIŞICU Ş. Phys Rev C, 2007, 76: 054609.
[14] ICHIKAWA T, HAGINO K, IWAMOTO A. Phys Rev Lett, 2009, 103: 202701.
[15] ICHIKAWA T. Phys Rev C, 2015, 92: 064604.
[16] ICHIKAWA T, MATSUYANAGI K. Phys Rev C, 2013, 88: 011602(R).
[17] ICHIKAWA T, MATSUYANAGI K. Phys Rev C, 2015, 92: 021602(R).
[18] DASGUPTA M, HINDE D J, DIAZ-TORRES A, et al. Phys Rev Lett, 2007, 99: 192701.
[19] LIN C J. Phys Rev Lett, 2003, 91: 229201.
[20] ICHIKAWA T, HAGINO K, IWAMOTO A. Phys Rev C, 2007, 75: 064612.
[21] HAGINO K, WATANABE Y. Phys Rev C, 2007, 76: 021601(R).
[22] DIAZ-TORRES A, HINDE D J, DASGUPTA, et al. Phys Rev C, 2008, 78: 064604.
[23] DIAZ-TORRES A. Phys Rev C, 2010, 82: 054617.
[24] UMAR A S, OBERACKER V E. Phys Rev C, 2006, 74: 021601(R).
[25] UMAR A S, SIMENEL C, OBERACKER V E. Phys Rev C, 2014, 89: 034611.
[26] DENISOV V YU. Phys Rev C, 2014, 89: 044604.
[27] DENISOV V YU. Phys Rev C, 2015, 91: 024603.
[28] CHENG K X, XU C. Phys Rev C, 2019, 99: 014607.
[29] CHENG K X, XU C. Phys Rev C, 2020, 102: 014619.
[30] RÖPKE G, SHUCK P, FUNAKI Y, et al. Phys Rev C, 2014, 90: 034304.
[31] XU C, REN Z Z, RÖPKE G, et al. Phys Rev C, 2016, 93: 011306(R).
[32] XU C, RÖPKE G, SCHUCK P, et al. Phys Rev C, 2017, 95: 061306(R).
[33] YANG S, XU C, RÖPKE G, et al. Phys Rev C, 2020, 101: 024316.
[34] RÖPKE G. Nucl Phys A, 2011, 867: 66.
[35] HAGINO K, TAKIGAWA N. Prog Theor Phys, 2012, 128: 1061.
[36] WINTHER A. Nucl Phys A, 1995, 594: 203.

[37] ŚWIĄTECKI W J, SIWEK-WILCZYŃSKA K, WILCZYŃSKI J. Acta Phys Pol B, 2003, 34: 2049.
[38] ŚWIĄTECKI W J, SIWEK-WILCZYŃSKA K, WILCZYŃSKI J. Phys Rev C, 2005, 71: 014602.
[39] CAP T, SIWEK-WILCZYŃSKA K, WILCZYŃSKI J. Phys Rev C, 2011, 83: 054602.
[40] SIWEK-WILCZYŃSKA K, CAP T, KOWAL M. Phys Rev C, 2019, 99: 054603.
[41] PURI P K, GUPTA R K. J Phys G: Nucl Part Phys, 1992, 18: 903.
[42] GHOSI O N, GHARAEI R. Phys Rev C, 2013, 88: 05467.
[43] CHENG K X, XU C. Nucl Phys A, 2019, 992: 121642.
[44] JIANG C L, REHM K E, JANSSENS R V F, et al. Phys Rev Lett, 2004, 93: 012701.
[45] JIANG C L, STEFANINI A M, ESBENSEN H, et al. Phys Rev Lett, 2014, 113: 022701.
[46] MORSAD A, KOLATA J J, TIGHE R J, et al. Phys Rev C, 1990, 41: 988.
[47] BACK B B, ESBENSEN H, JIANG C L, et al. Rev Mod Phys, 2014, 86: 317.
[48] KELLER J G, SCHMIDT K H, HESSBERGER F P, et al. Nucl Phys A, 1986, 452: 173.
[49] STEFANINI A M, BEHERA B R, BEGHINI S, et al. Phys Rev C, 2007, 76: 014610.
[50] BECKERMAN M, SALOMAA M, SPERDUTO A, et al. Phys Rev C, 1982, 25: 837.
[51] STEFANINI A M, MONTAGNOLI G, ESBENSEN H, et al. Phys Rev C, 2017, 96: 014603.
[52] STEFANINI A M, MONTAGNILI G, CORRADI L, et al. Phys Rev C, 2010, 82: 014614.
[53] MUKHERJEE A, DASGUPTA M, HINDE D J, et al. Phys Rev C, 2002, 66: 034607.
[54] STEFANINI A M, MONTAGNOLI G, SILVESTRI R. Phys Lett B, 2009, 679: 95.
[55] JIANG C L, STEFANINI A M, ESBENSEN H. Phys Rev C, 2010, 82: 041601(R).
[56] MONTAGNOLI G, STEFANINI A M, JIANG C L, et al. Phys Rev C, 2012, 85: 024607.
[57] JIANG C L, BACK B B, ESBENSEN H, et al. Phys Rev C, 2006, 73: 014613.
[58] SHRIVASTAVA A, MAHATA K, PANDIT S K, et al. Phys Lett B, 2016, 755: 322.
[59] SHRIVASTAVA A, MAHATA K, NANAL V, et al. Phys Rev C, 2017, 96: 034620.
[60] JIANG C L, BACK B B, ESBENSEN H, et al. Phys Rev C, 2008, 78: 017601.
[61] MONTAGNOLI G, STEFANINI A M, JIANG C L, et al. Phys Rev C, 2018, 97: 024610.
[62] SEKIZAWA K, HAGINO K. Phys Rev C, 2019, 99: 051602(R).

极深垒下熔合反应中扩散过程的研究

程凯旋, 许 昌†

(南京大学物理系，南京 210093)

摘要: 基于弹核和靶核接触后的泡利阻塞效应，引入了一个新的扩散因子来描述在极深垒下能区熔合反应中的阻碍现象。在本工作中，熔合截面假定由两部分的乘积构成：克服库仑势垒的隧穿因子和两个反应核接触后的扩散因子。前者可以由耦合道方法来描述，后者则由入射的能量和系统的温度决定。对存在阻碍现象的21个熔合体系进行了详细分析，发现扩散因子在熔合阻碍的实验阈值能量附近起到了重要的作用。此外，以负 Q 值熔合体系 ^{64}Ni+^{64}Ni 和正 Q 值熔合体系 ^{24}Mg+^{30}Si 为例，发现熔合截面以及两个重要表象 (天体 S 因子和对数导数) 的计算结果与实验数据具有较好的一致性。

关键词: 熔合阻碍；耦合道模型；扩散过程

收稿日期: 2020-06-23；　**修改日期:** 2020-07-23

基金项目: 国家自然科学基金资助项目 (11822503, 11575082); 中央高校基本科研专项资金项目 (南京大学)

† **通信作者:** 许昌，E-mail: cxu@nju.edu.cn。